Tumor microenvironment remodeling enables bypass of oncogenic KRAS dependency in pancreatic cancer

Pingping Hou, Avnish Kapoor, Qiang Zhang, Jiexi Li, Chang-Jiun Wu, Jun Li, Zhengdao Lan, Ming Tang, Xingdi Ma, Jeffrey J. Ackroyd, Raghu Kalluri, Jianhua Zhang, Shan Jiang, Denise J. Spring, Y. Alan Wang, and Ronald A. DePinho

Supplementary Figures S1-S9

Supplementary Figure 1

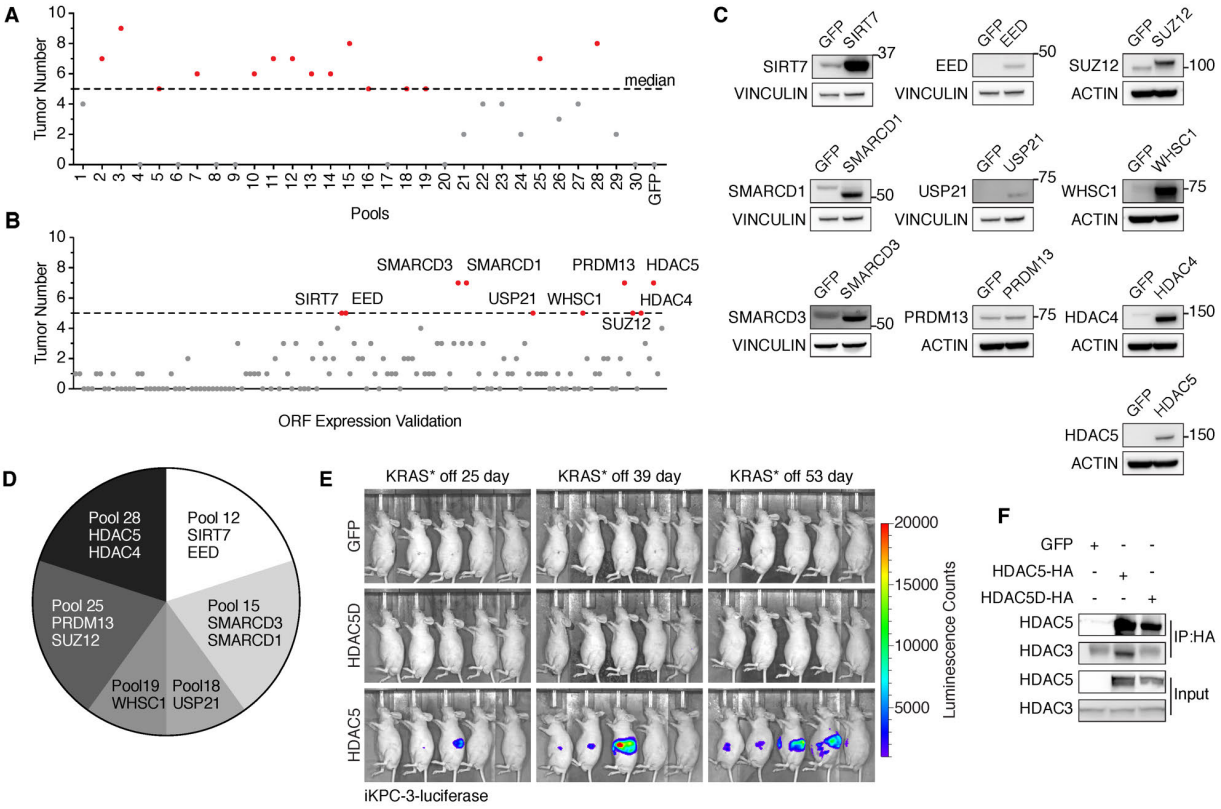

G

HDAC Family	ORF ID	Primary Screen (N=10)		Validation
		Pool ID (tumor #)	Enrichment	(N=5)
Class I	HDAC1	Pool 15 (8 tumors)	3	-
	HDAC2	-	-	-
	HDAC3	Pool 14 (6 tumors)	1	-
	HDAC8	Pool 11 (7 tumors)	0	-
Class IIa	HDAC4	Pool 28 (8 tumors)	5	1
	HDAC5	Pool 28 (8 tumors)	7	5
	HDAC7	Pool 22 (4 tumors)	-	-
	HDAC9	Pool 23 (4 tumors)	-	-
Class IIb	HDAC6	Pool 22/23 (4 tumors)	-	-
	HDAC10	Pool 25 (7 tumors)	2	-
Class IV	HDAC11	Pool 10 (6 tumors)	1	-

Supplementary Figure 1. Epigenetic library screening to bypass KRAS* dependency. A, KRAS*-independent escaper tumor numbers generated from 10 mice with orthotopically transplanted iKPC cells for each pool. Fifteen red color highlighted pools promoted the generation of more than 5 escapers and were further validated for enriched ORF expression. **B**, Validation of ORF enrichment in escaper tumors. Gene expression in escapers from 15 highlighted pools in (A) were analyzed by qRT-PCR. ORFs with gene expression levels higher in escapers than in "input" iKPC cells were considered "enriched". The top 10 ORFs enriched in more than 5 escaper tumors are highlighted. **C**, Validation of the overexpressed top 10 gene candidates in iKPC-1 cells by western blot analysis. **D**, Distribution of the top 10 ORFs in screening sub-pools. **E**, BLI imaging

of nude mice orthotopically transplanted with GFP-, HDAC5- or HDAC5D-overexpressed (OE) iKPC-3 cells with luciferase reporter. **F**, Mutation of *HDAC5* (HDAC5D) interrupted HDAC5-HDAC3 interaction to form functional repressive complex by co-IP analysis. **G**, The capability of HDAC family members to bypass KRAS* dependency extracted from ORF screening.

Supplementary Figure 2

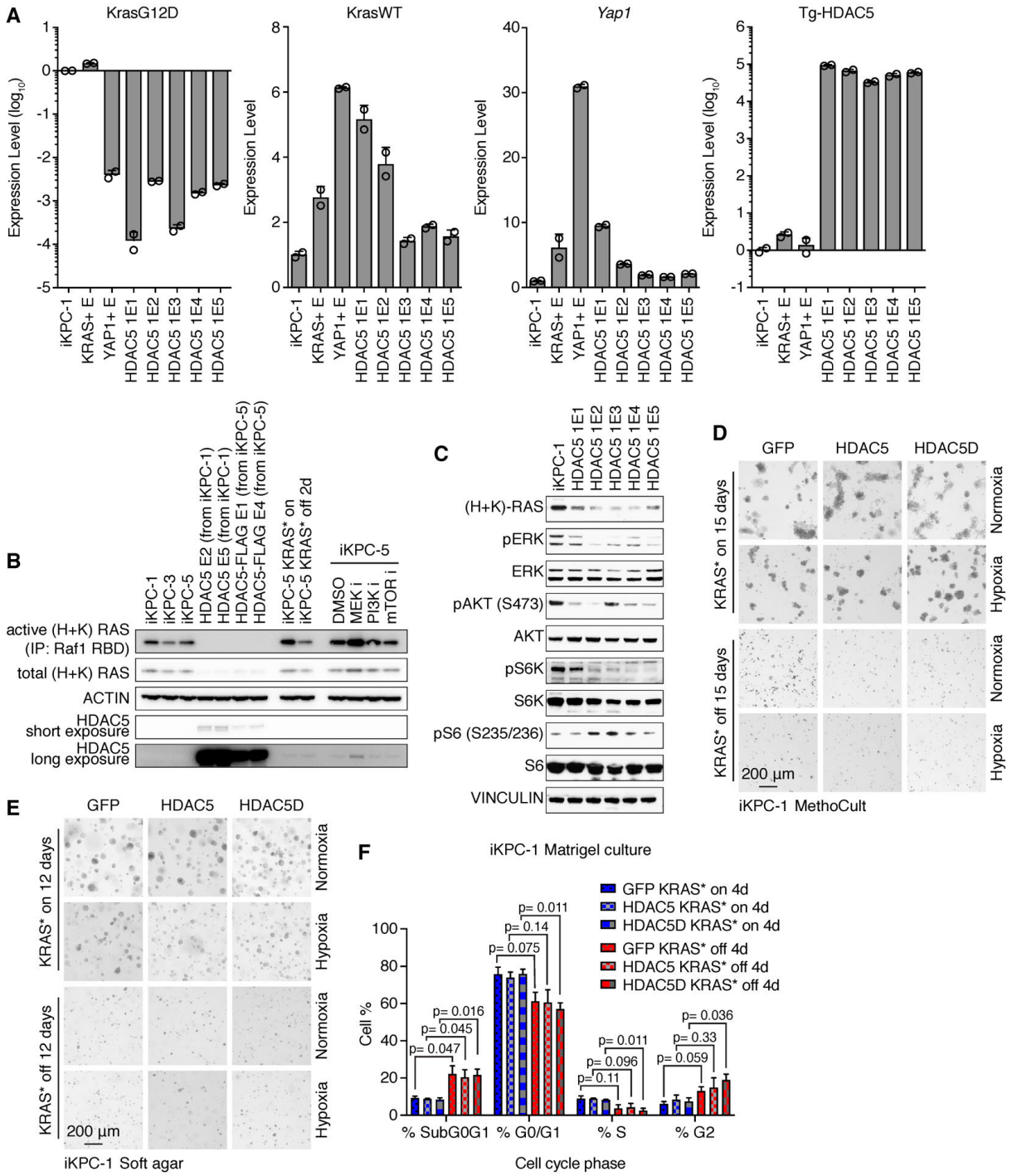

Supplementary Figure 2. Characterization of *HDAC5* escapers. A, Validation of gene expression of endogenous *Kras*, transgenic KRAS*, *Yap1*, and transgenic *HDAC5* (Tg-HDAC5) by qRT-PCR in *HDAC5* escaper cells. KRAS*-reactivated escaper cells and *Yap1*-amplified escaper cells were served as positive controls. Data are represented as mean ± SD. **B**,

Determination of RAS activity in primary iKPC cells, *HDAC5* escapers, KRAS* on and off iKPC-5 cells, and iKPC-5 cells after inhibition of KRAS* downstream pathways. Active RAS was pulled down by agarose beads crosslinked with Ras-binding domain (RBD) of Raf1, and detected by (H+K) RAS antibody. **C**, Validation of KRAS* downstream signaling pathways in *HDAC5* escaper cells by western blot analysis. **D**-**E**, The 3-D colony formation assay of GFP-, HDAC5- or HDAC5D-OE iKPC-1 cells after KRAS* extinction in MethoCult (D) or soft agar (E) culture under normoxia or hypoxia conditions. KRAS*-expressing cells were used as positive control. **F**, Cell cycle analysis of iKPC-1 cells with or without KRAS* expression in Matrigel culture *in vitro*. The iKPC-1 cells overexpressing GFP, HDAC5 or HDAC5D were seeded in Matrigel with or without DOX treatment, and collected after 4 days for propidium iodide staining. Three independent experiments were performed for statistical analysis. Two-tailed unpaired t tests were performed to calculate the p values.

Supplementary Figure 3

A

Pathway	Receptor	Ligand	Ligand type	Ligand Gene ID	Relative expression of ligands versus Actin (ave x1000)		Fold Change (Tumor vs Cells)	Tested ligands/ pathway activators
					KRAS-extincted tumors for 24hrs	HDAC5 escaper cells		
TGFβ	TGFBR3	TGFβ1	Cytokine	Tgfb1	13.5	3.4	3.97	TGFβ1
		TGFβ2	Cytokine	Tgfb2	1.4	1.6	0.88	
		TGFβ3	Cytokine	Tgfb3	7.6	6.5	1.17	
GPCR	PTGFR	PGF2α	Prostaglandin	n/a	n/a	n/a	n/a	PGF2α
FGFR	FGFR1	FGF1	Cytokine	Fgf1	12	0.007	1714.29	FGF1
PDGFR	PDGFRB	PDGFAB	Cytokine	Pdgfb	11.4	0.4	28.50	PDGFBB
		PDGFBB	Cytokine					
		PDGFCC	Cytokine	Pdgfd	3.8	0.01	380.00	
		PDGFDD	Cytokine					
PDGFR	PDGFRA	PDGFAA	Cytokine	Pdgfa	14.2	6.2	2.29	PDGFAA
		PDGFAB	Cytokine					
		PDGFBB	Cytokine	Pdgfc	4.5	8	0.56	
		PDGFCC	Cytokine					
Wnt	FZD2/3/8/9	WNT2	Cytokine	Wnt2	1.1	0.007	157.14	WNT5a
		WNT3	Cytokine	Wnt3	0.12	0	n/a	
		WNT5a	Cytokine	Wnt5a	2.7	0.5	5.40	
		WNT11	Cytokine	Wnt11	0.45	0.07	6.43	
GPCR	LPAR1	Lysophosphatidic Acid (LPA)	Phospholipid	n/a	n/a	n/a	n/a	LPA
JAK/STAT	IL6RA	IL6	Cytokine	Il6	0.56	0.0007	800.00	IL6
GPCR	S1PR1/2	S1P	Sphingolipid	n/a	n/a	n/a	n/a	S1P
JAK/STAT	IL6ST	IL6	Cytokine	Il6	0.56	0.0007	800.00	IL6
		LIF	Cytokine	Lif	3	0.5	6.00	
		CTF1	Cytokine	Ctf1	1.4	0.37	3.78	
		IL11	Cytokine	Il11	1.2	0.3	4.00	
RAR/RXR	RARB/G	Retinoic Acid (RA)	Chemical	n/a	n/a	n/a	n/a	Adapalene
Hedgehog	SMO	IHH	Cytokine	Ihh	16.8	0.005	3360.00	SAG
RAR/RXR	RXRB	RA	Chemical	n/a	n/a	n/a	n/a	Adapalene
		All-trans Retinoic Acid (ATRA)	Chemical	n/a	n/a	n/a	n/a	

B

Condition	Colony per 500 cells		Condition	Colony per 500 cells	
	HDAC5	HDAC5D		HDAC5	HDAC5D
Untreated control	0	0	FGF1 5ng/ml	0	0
Untreated control	0	0	FGF1 10ng/ml	0	0
PDGFAA 10ng/ml	0	0	LPA 1μM	0	0
PDGFAA 30ng/ml	0	0	LPA 5μM	0	0
PDGFAA 50ng/ml	1	0	LPA 10μM	0	0
PDGFBB 10ng/ml	0	0	PGF2α 125nM	0	0
PDGFBB 30ng/ml	0	0	PGF2α 250nM	0	0
PDGFBB 50ng/ml	0	0	S1P 2μM	0	0
IL-6 0.1ng/ml	0	0	S1P 5μM	0	0
IL-6 0.5ng/ml	1	0	Adepelene 10μM	0	0
IL-6 1ng/ml	0	0	Adapalene 20μM	0	0
WNT5a 0.25μg/ml	0	0	TGFβ1 0.5ng/ml	29	24
WNT5a 0.5μg/ml	1	0	SAG 10nM	0	0
FGF1 1ng/ml	0	0			

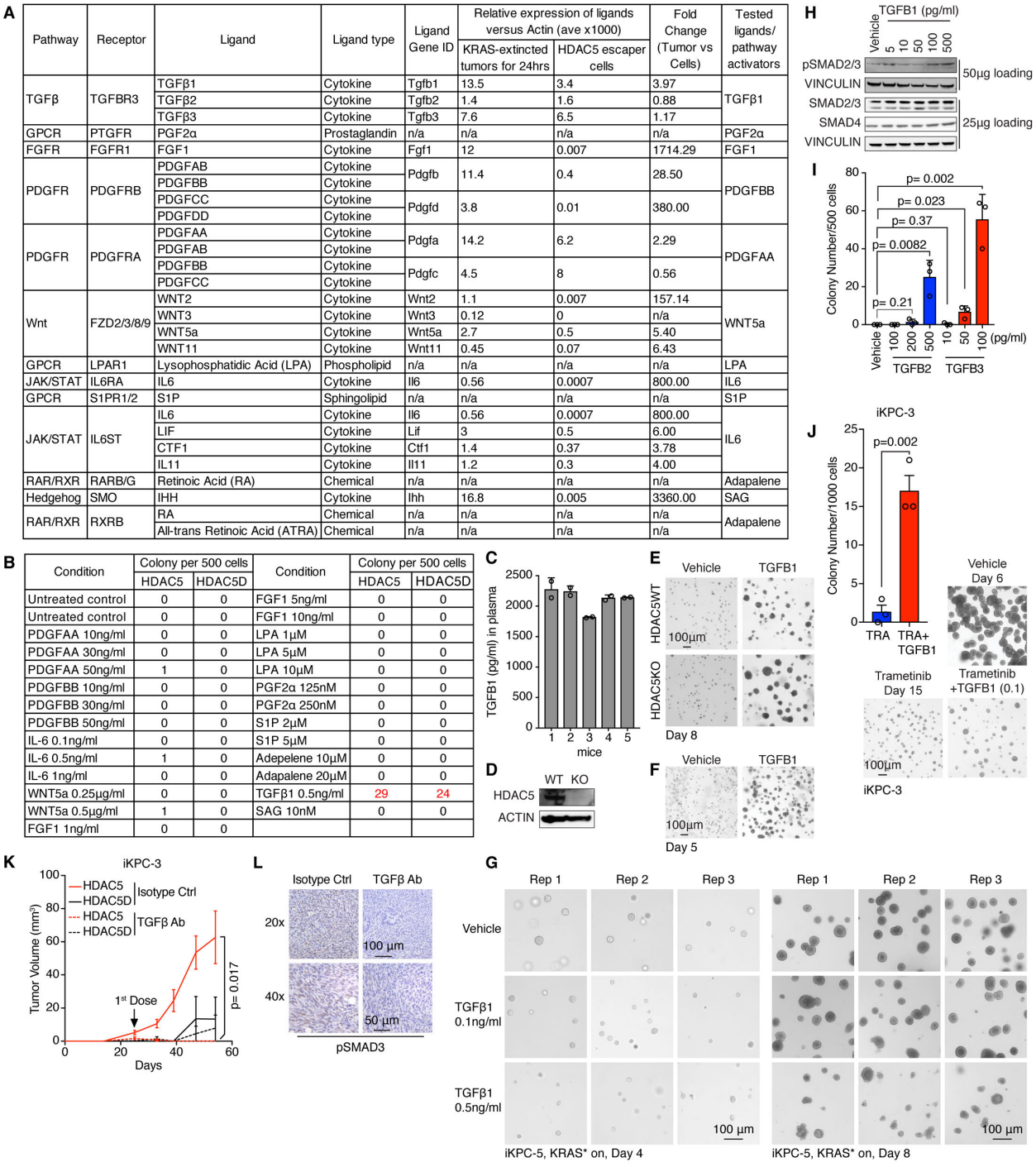

Supplementary Figure 3. Activation of the TGFβ pathway promotes pancreatic cancer cells to bypass KRAS* dependency. A, Summary of 18 candidate receptors, corresponding ligands and small molecule activators/cytokines. **B,** Experimental design and summary of the screening results of the 13 small molecule activators or cytokines to bypass KRAS* dependency in iKPC-3

cells. Colonies were counted at Day 9 after KRAS* extinction. **C,** TGFβ1 concentration in 5 mouse plasma samples. **D,** Validation of *Hdac5* knockout in iKPC-5 cells by western blot analysis. **E,** TGFβ1 (0.5 ng/ml) drove KRAS*-independent colony growth after KRAS* extinction in *Hdac5* wildtype and *Hdac5* knockout iKPC cells. Images were taken at Day 8 after KRAS* extinction. **F,** TGFβ1 (0.5 ng/ml) drove KRAS*-independent colony growth after KRAS* extinction in iKPC-1 cells. Images were taken at Day 5 after KRAS* extinction. **G**, TGFβ treatment attenuated colony growth of KRAS*-expressing iKPC-5 cells in 3-D culture. **H,** Activation of pSMAD2/3 in iKPC cells after TGFβ1 treatment at indicated concentrations by western blot analysis. **I,** TGFβ2 and TGFβ3 drove iKPC-3 cells to bypass KRAS* dependency in Matrigel culture (n = 3). Colonies were counted at Day 9 after KRAS* extinction. **J**, TGFβ1 promoted MEK inhibition (Trametinib, 50 nM)-resistant iKPC-3 colony growth at Day 15 (n = 3). Representative images and colony number quantification are shown. **K,** Another independent experiment showing that neutralization of TGFβ impaired KRAS*-independent tumor growth of *HDAC5*-OE iKPC-5 cells subcutaneously transplanted in nude mice (n = 3). **L**, IHC staining of pSMAD3 in tumors from isotype control group and TGFβ neutralizing antibody treatment group related to Fig. 2F. For I, J and K, data are represented as mean ± SEM, and two-tailed unpaired t tests were performed to calculate the p values.

Supplementary Figure 4

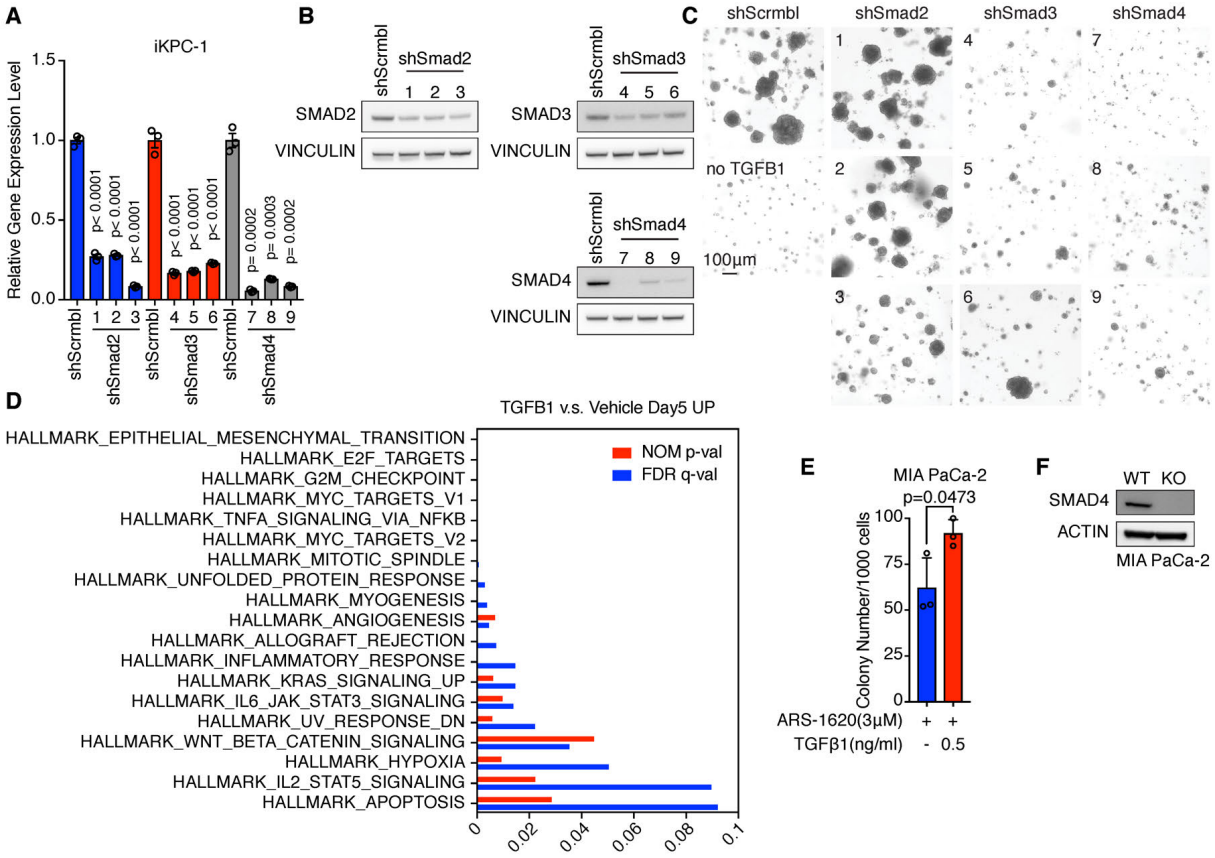

Supplementary Figure 4. Necessity of the canonical TGFβ pathway to promote pancreatic cancer cells to bypass KRAS* dependency. A and **B,** Validation of knockdown efficiency of *Smad2*, *Smad3* and *Smad4* shRNAs in iKPC-1 cells by qRT-PCR (A) and western blot (B) analysis. **C,** Representative images of TGFβ1-driven KRAS*-independent colony formation comparing scramble control and knockdown of *Smad2*, *Smad3* and *Smad4*. **D,** Gene signatures enriched in iKPC cells treated with TGFβ1 versus cells treated with vehicle control 5 days after KRAS* extinction in 3-D culture by GSEA analysis of RNA-seq data (n = 3 for each group). **E,** TGFβ promotes MIA PaCa-2 cells to get resistant to $KRAS^{G12C}$ inhibitor ARS-1620 treatment *in vitro*. Data are represented as mean ± SD. **F**, Validation of SMAD4 knockout in human MIA PaCa-2 cells by western blot analysis. For **A** and **E**, data are represented as mean ± SD, and two-tailed unpaired t tests were performed to calculate the p values.

Supplementary Figure 5

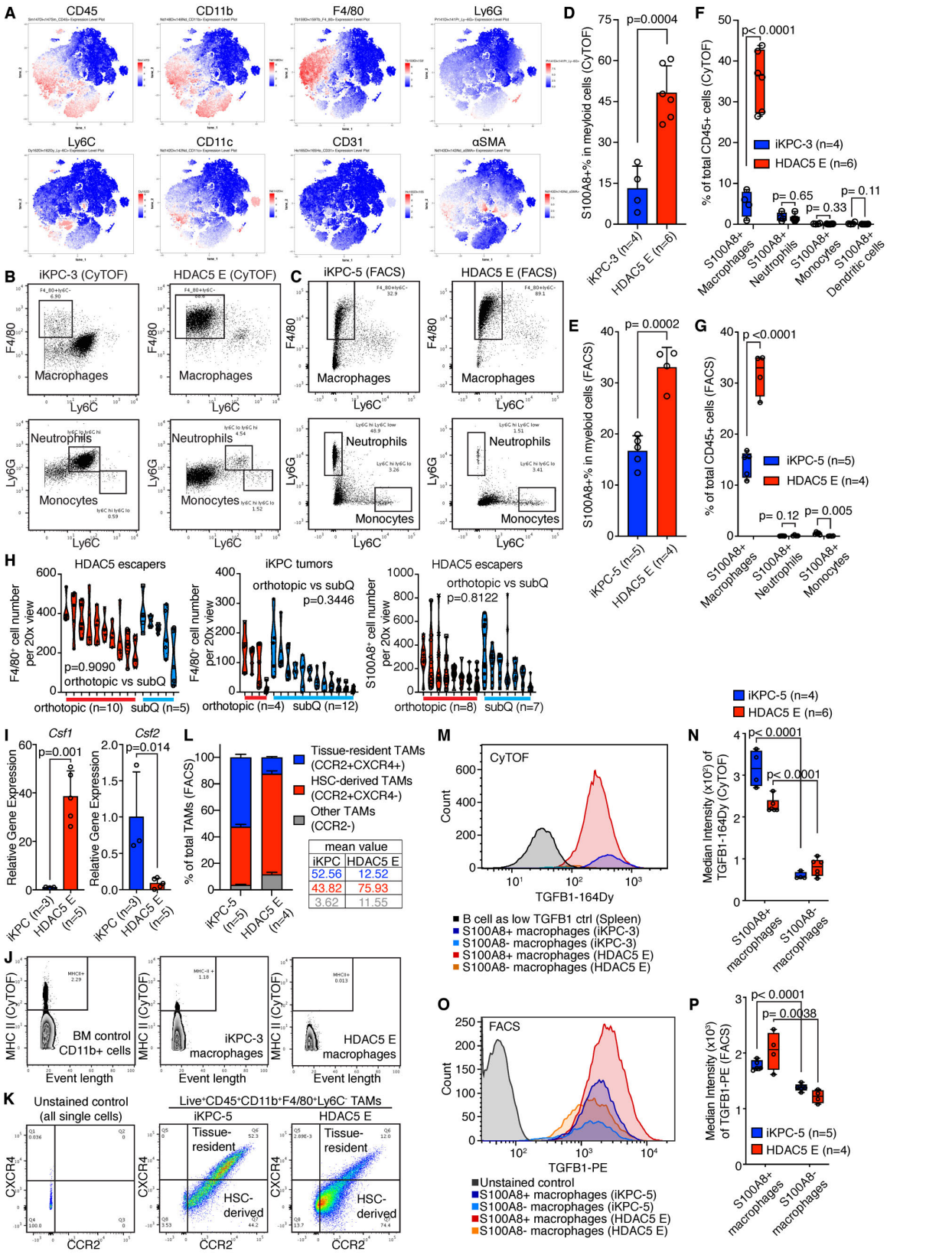

Supplementary Figure 5. Characterization of tumor-infiltrated immune cells. A, Expression distribution of lineage marker genes by tSNE plot analysis of CyTOF data related to Fig. 3A. **B** and **C,** Gates of macrophages, monocytes and neutrophils in a representative iKPC tumor and a *HDAC5*-driven escaper by CyTOF (B) and FACS (C) analysis. Data are displayed by FlowJo. $CD45^+CD11b^+F4/80^+Ly6C^-$ cells represented macrophages; $CD45^+CD11b^+F4/80^-Ly6G^{high}Ly6C^{low}$ cells represented neutrophils. $CD45^+CD11b^+F4/80^-Ly6G^{low}Ly6C^{high}$ cells represented monocytes. **D-E,** Percentage of $S100A8^+$ cells in myeloid cells comparing iKPC tumors and *HDAC5* escapers by CyTOF (D) and FACS (E) analysis. **F** and **G,** Percentage of different $S100A8^+$ myeloid cell types in iKPC tumors and *HDAC5* escapers by CyTOF (F) and FACS (G) analysis. **H**, Comparison of $F4/80^+$ cell numbers by IHC staining in different *HDAC5* escaper tumors (left) or iKPC primary tumors (middle) generated from subcutaneous and orthotopic allograft models; comparison of $S100A8^+$ cell numbers after IHC staining in different HDAC5 escapers (right) generated from subcutaneous and orthotopic allograft models. Two-tailed unpaired t tests between the orthotopic and subcutaneous (subQ) groups including all the samples were performed to calculate the p values. **I,** RNA expression of *Csf1* and *Csf2* in iKPC cells (n = 3) and *HDAC5* escaper cells (n = 5) by qRT-PCR analysis. **J**, Gates of the MHC II^+ cells in bone marrow (BM) myeloid cells and in macrophages from an iKPC-3 tumor and a *HDAC5* escaper by FlowJo analysis of the FACS data. **K**, Gates of tissue-resident and HSC-derived macrophages in a representative iKPC-5 tumor and a *HDAC5* escaper by FACS analysis. Data are displayed by FlowJo. $CXCR4^+CCR2^+$ macrophages represented tissue-resident TAMs; $CXCR4^-CCR2^+$ macrophages cells represented HSC-derived TAMs. **L**, Quantification of the tissue-resident, HSC-derived and other tumor associated macrophages (TAMs) in iKPC-5 primary tumors and *HDAC5* escapers from orthotopic allograft mouse model in nude mice. **M**, Representative overlaid histograms of TGFB1-164Dy intensity distribution in $S100A8^+$ and $S100A8^-$ macrophages from HDAC5 escapers and primary tumors, which were generated from subcutaneous allograft models in nude mice. B cells expressed low TGFB1 in our models, so we used the histogram of TGFB1-164Dy intensity distribution in B cells from spleen as the control for low TGFB1 expressing cells. **N**, The quantification of TGFB1-164Dy median intensities in $S100A8^+$ and $S100A8^-$ macrophages from HDAC5 escapers and primary tumors, which were generated from subcutaneous allograft models in nude mice. **O**, Representative overlaid histograms of TGFB1-PE intensity distribution in $S100A8^+$ and $S100A8^-$ macrophages from HDAC5 escapers and primary tumors, which were generated from orthotopic allograft models in nude mice. Unstained cells were used as negative

TGFB1 control. **P**, The quantification of TGFB1-PE median intensities in $S100A8^+$ and $S100A8^-$ macrophages from HDAC5 escapers and primary tumors, which were generated from orthotopic allograft models in nude mice. For **D**, **E** and **L**, data are represented as mean ± SEM. For **I**, data are represented as mean ± SD. For **D**-**G**, **I**, **N** and **P**, two-tailed unpaired t tests were performed to calculate the p values.

Supplementary Figure 6

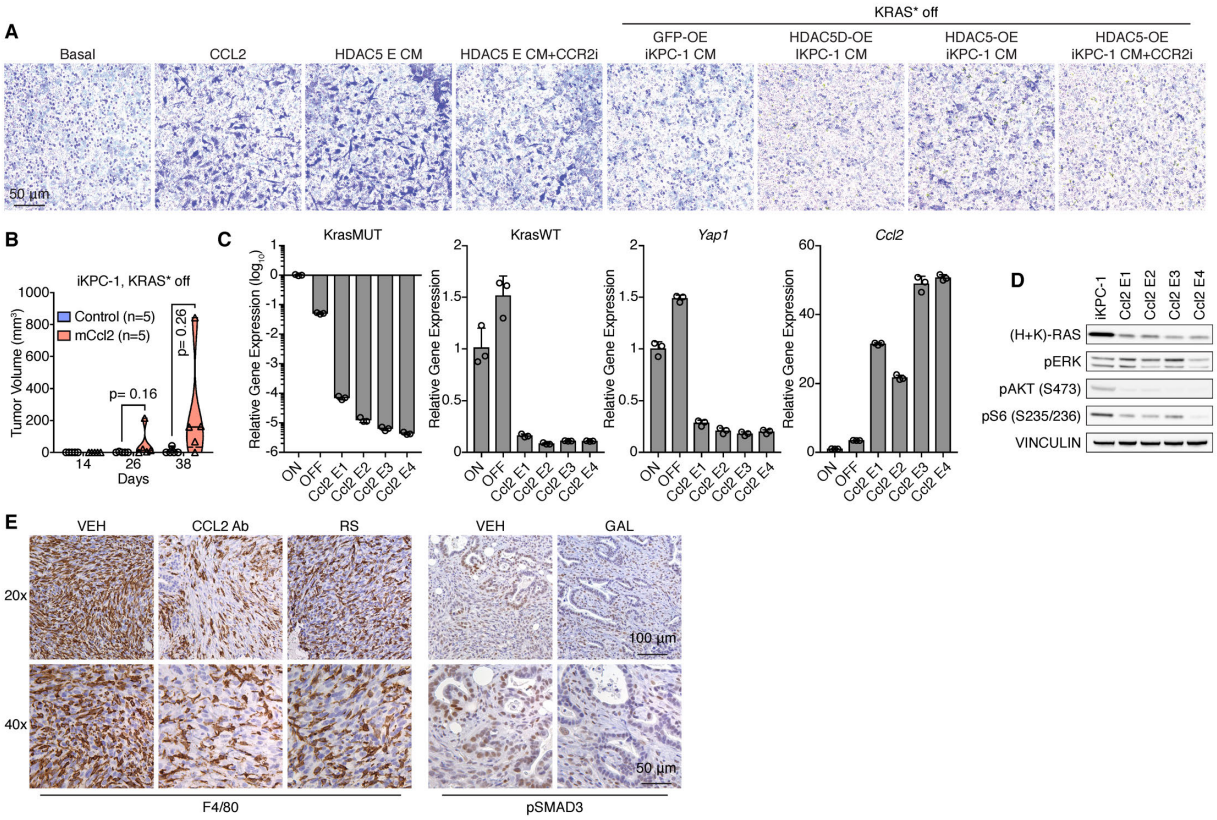

Supplementary Figure 6. Overexpression of *HDAC5* in iKPC cells promotes macrophage infiltration via CCL2/CCR2 axis. **A**, Representative images of migrated macrophages in transwell assay quantified in Fig. 4C and 4D. **B**, Tumor growth analysis comparing iKPC-1 cells overexpressing GFP w/o Doxy feeding and *Ccl2* w/o Doxy feeding in subcutaneous allograft model in nude mice (n=5 for each group). Two-tailed unpaired t tests were performed to calculate the p values. **C**, Validation of gene expression of endogenous *Kras*, transgenic KRAS*, *Yap1*, and *Ccl2* by qRT-PCR in *Ccl2* escapers. The KRAS*-expressing iKPC-1 tumor and iKPC-1 tumor after KRAS* extinction for 3 days were served as positive and negative controls, respectively. Data are represented as mean ± SD. **D**, Validation of KRAS* downstream signaling pathways in *Ccl2* escaper cells by western blot analysis. **E**, Related to Fig. 4I, CCR2 inhibitor RS 504393 (RS) and CCL2 neutralizing antibody (CCL2 Ab) attenuated macrophage infiltration into tumors by IHC analysis of F4/80 compared to vehicle control (VEH); TGFBR inhibitor Galunisertib (GAL) inhibited TGFβ pathway activation in tumor cells by IHC analysis of pSMAD3 compared to vehicle control (VEH).

Supplementary Figure 7

A

ID	Anotation	Rank 1 by p-value (HDAC5 E vs iKPC)	Rank 2 by p-value (KD vs Scrmbl)	Rank 1+ Rank 2
Zfp36	zinc finger protein 36	4	3	7
Pnrc1	proline-rich nuclear receptor coactivator 1	11	2	13
Btg2	BTG family, member 2	12	1	13
Socs3	suppressor of cytokine signaling 3	5	9	14
Lif	leukemia inhibitory factor	8	6	14
Hes1	hairy and enhancer of split 1	1	14	15
Hbegf	heparin-binding EGF-like growth factor	3	13	16
Dusp5	dual specificity phosphatase 5	6	11	17
Sdc4	syndecan 4	9	8	17
Phlda1	pleckstrin homology-like domain, family A, member 1	7	12	19
Junb	jun B proto-oncogene	14	5	19
Smad3	SMAD family member 3	2	17	19
Tnip1	TNFAIP3 interacting protein 1	17	4	21
Ifngr2	interferon gamma receptor 2	16	7	23
Atp2b1	ATPase, Ca++ transporting, plasma membrane 1	15	10	25
F3	coagulation factor III	10	16	26
Trib1	tribbles homolog 1	13	15	28

DEGs: differentially expressed genes; KD: knockdown.

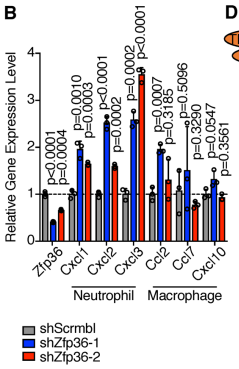

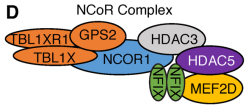

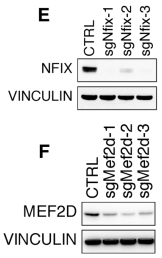

C

Protein FDR Confidence	Protein ID	Accession	Coverage [%]	# PSMs	MW [kDa]	Abundance: co-IP: FLAG Rep1	co-IP: FLAG Rep2	co-IP: IgG Rep1	co-IP: IgG Rep2	Ratio (FLAG/IgG)	Classification
High	HDAC5 (bait)	B7ZDF7	34	277	119.8	1168810194	1020002655	2122054	1723578	569.2	NCoR HDAC3 Complex
High	TBL1X	Q9QXE7	38	24	56.8	6049234	6466067	437962	539705	12.8	NCoR HDAC3 Complex
High	TBL1XR1	Q8BHJ5	21	14	55.6	646176	666927			/	NCoR HDAC3 Complex
High	NCOR1	Q5RIM6	12	24	270.6	3468565	3470502	225679	135608	19.2	NCoR HDAC3 Complex
High	NCOR1	E9Q2B2	12	23	263.9	325135	496510			/	NCoR HDAC3 Complex
High	HDAC3	Q3UM33	10	4	48.8	1468902	1071053			/	NCoR HDAC3 Complex
High	GPS2	Q921N8	7	2	36.7	498714	322838		28568	28.8	NCoR HDAC3 Complex
High	HDAC9	A0A1B0GSQ5	4	53	116.7	79472115	83178050	1735006	274067	81.0	NCoR HDAC3 Complex
High	HDAC4	Q6NZM9	3	14	118.5	18133182	19086712			/	NCoR HDAC3 Complex
High	SAP18	E9Q317	29	6	19.6	1178745	1873093	21270	167592	16.2	SIN3/HDAC1/2 complex
High	TRIM28	Q62318	5	11	88.8	1088103.406	658482.2656	81503.78125		21.4	NuRD/SETDB1
High	NFIX	E9PUH7	7	2	54.1	38296	218919			/	Nuclear Factor
High	MEF2D	Q63943	4	3	55	610572	886563			/	Transcription Factor
High	CAMK2D	A0A0G2JGS4	12	9	60	1941199.211	1704992.949	163926.7324	93219.98438	14.2	CaM Kinase

Supplementary Figure 7. *HDAC5* regulates expression of macrophage-recruiting chemokines through *Socs3*. A, Exploration of *HDAC5* targets by overlapping 3 profiling datasets as described in Fig. 5A. Seventeen candidate genes were filtered out and ranked by p-values in the 2 RNA-seq datasets from low to high. **B,** Gene expression of neutrophil- and macrophage-attracted chemokines after knockdown of *Zfp36* in iKPC cells. Data are represented as mean ± SD, and two-tailed unpaired t tests were performed to calculate the p values. **C**, Identification of potential HDAC5 interactors by co-IP/MS analysis. **D**, Schematic model of the potential HDAC5 co-repressor complex. **E** and **F**, Validation of knockdown efficiency of *Nfix* (E) and *Mef2d* (F) using CRISPR/Cas9 in HDAC5 escaper cells by western blot analysis.

Supplementary Figure 8

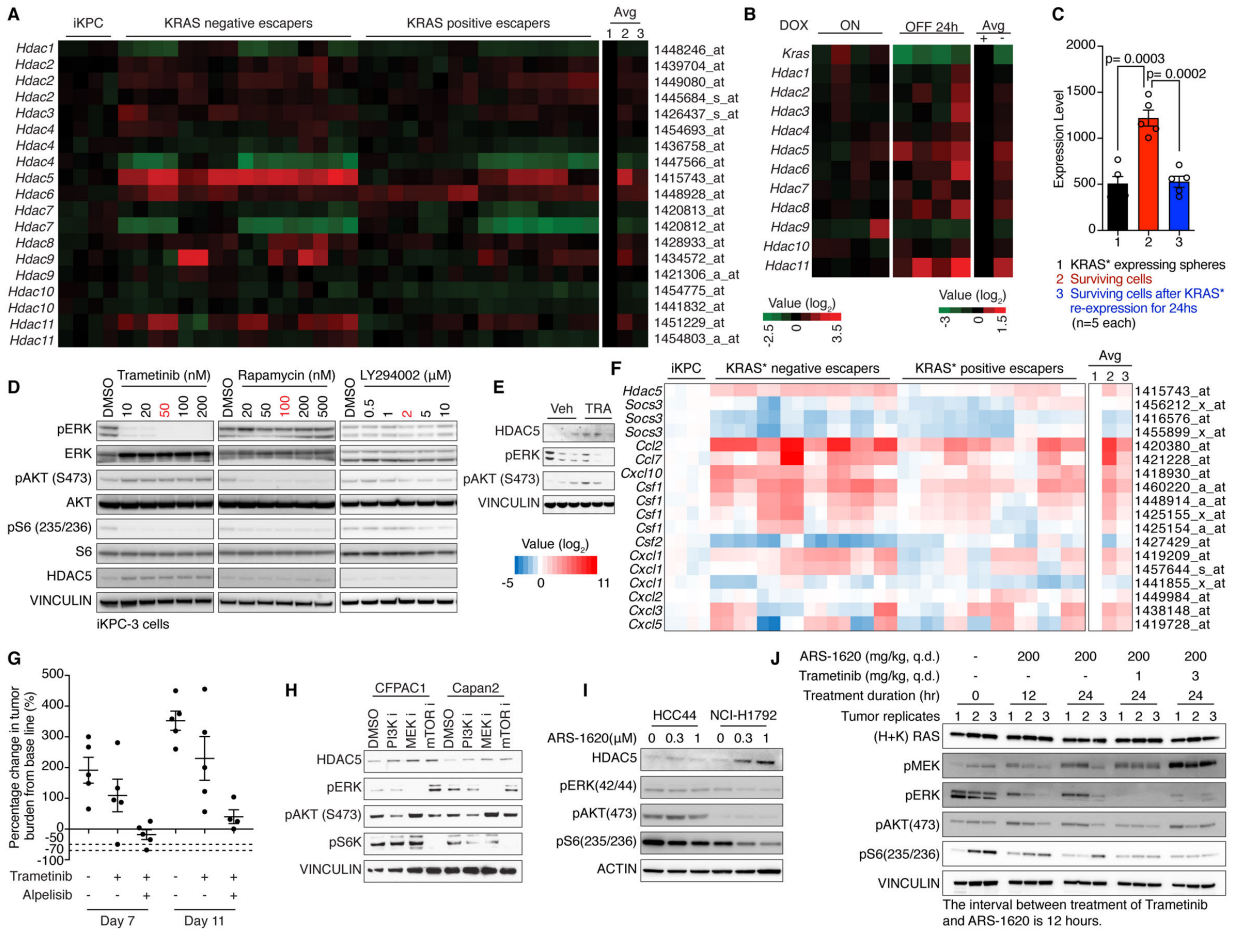

Supplementary Figure 8. HDAC5 is upregulated after inhibition of the KRAS*/MAPK pathway in *de novo* generated escapers and human PDAC lines. A, Hdac expression in iKPC tumors, *de novo* generated KRAS* negative escapers and KRAS* reactivated escapers. "1", "2" and "3" are representing "iKPC cells", "KRAS*-negative escapers" and "KRAS*-positive escapers", representatively. **B,** Hdac expression in KRAS*-expressing iKPC tumor samples and samples 24 hours after KRAS* extinction. **C,** *Hdac5* is upregulated in surviving cells. Two-tailed unpaired t tests were performed to calculate the p values. **D**, Dosage titration and on-target effect determination of MEK inhibitor Trametinib, mTOR inhibitor Rapamycin, and PI3Ka inhibitor LY294002 in iKPC-3 cells by western blot analysis. The red- highlighted concentrations were chosen for molecular and functional analysis *in vitro*. **E,** HDAC5 is upregulated in transplanted iKPC tumors after Trametinib (TRA) treatment. **F**, RNA expression of chemokines and cytokines that chemoattract macrophages and neutrophils in iKPC cells, KRAS*-negative escapers and KRAS*-positive escapers. "1", "2" and "3" represent "iKPC cells", "KRAS*-negative escapers"

and “KRAS*-positive escapers”, representatively. **G,** Comparison of tumor growth between vehicle control, MEK inhibitor Trametinib only and dual inhibition of MEK by Trametinib and PI3Kα by Alpelisib in transplanted syngeneic iKPC tumors (*n* = 7). Tumor sizes were measured at Day 7 and Day 11 post-treatment. Data are represented as mean ± SEM. **H,** Western blot analysis shows regulation of HDAC5 expression by KRAS* downstream signaling pathways in human PDAC cell lines. **I,** Western blot analysis shows upregulation of HDAC5 expression by $KRAS^{G12C}$ inhibitor ARS-1620 in human NSCLC cell lines with $KRAS^{G12C}$ mutation. **J**, Related to Fig. 6J, pharmacodynamic determination of $KRAS^{G12C}$ inhibitor ARS-1620 alone and in combination with MEK inhibitor Trametinib in MIA PaCa-2 xenograft tumors in nude mice.

Supplementary Figure 9

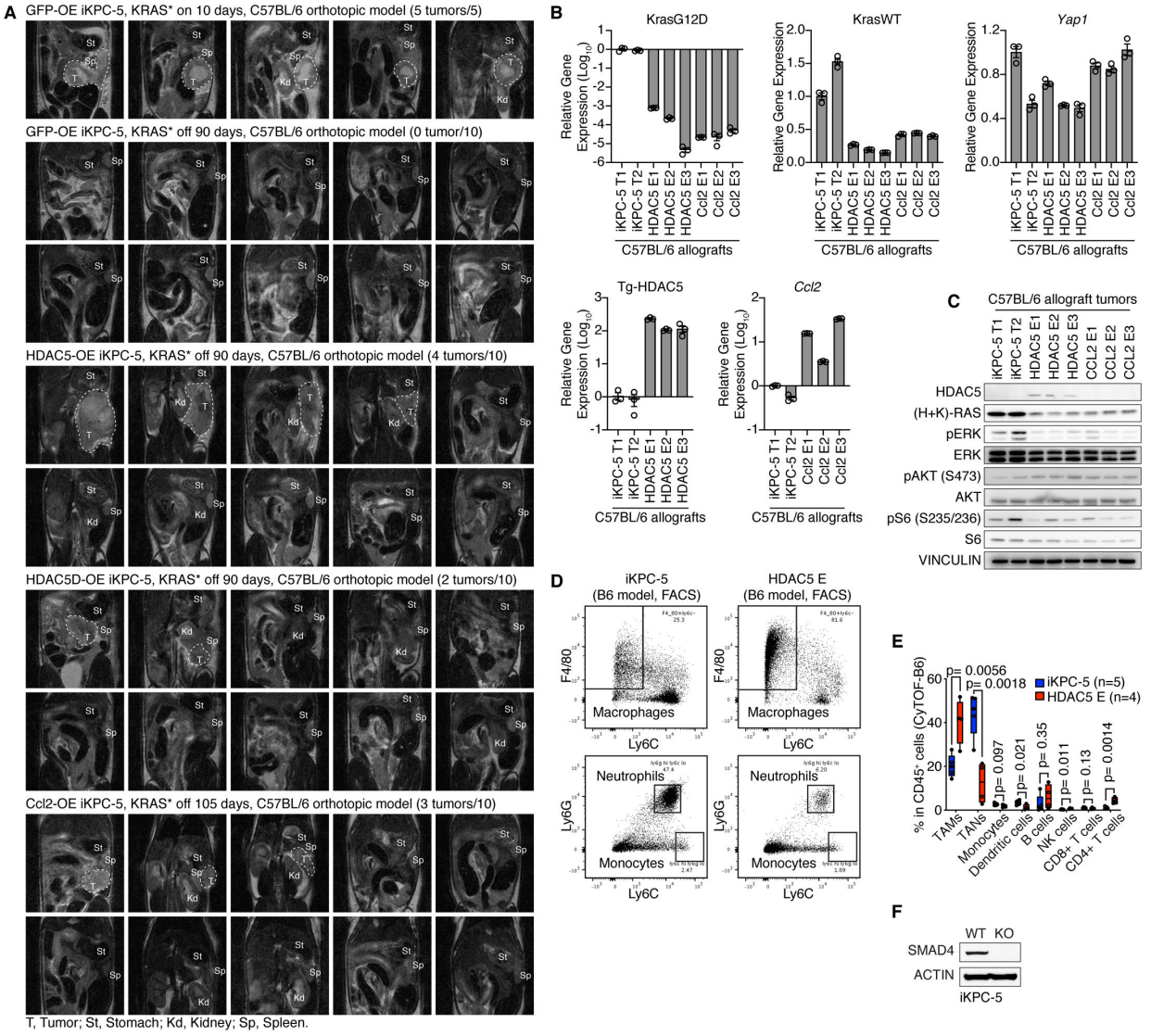

Supplementary Figure 9. Characterization of *HDAC5* escapers generated in syngeneic mouse models. A, MRI images to examine the tumor burden of orthotopically transplanted GFP-, *HDAC5*-, HDAC5D and *Ccl2*-OE iKPC-5 cells in C57BL/6 mice after KRAS* extinction at indicated days. MRI images of KRAS*-expressing GFP-OE iKPC-5 tumors were used as positive control. **B**, Transcriptional expression of KRAS*, endogenous *Kras*, endogenous *Yap1*, transgenic HDAC5 and total *Ccl2* in *HDAC5* and *Ccl2* escapers by qRT-PCR analysis. The iKPC tumors were used as control. **C**, Activation of KRAS* signaling pathway in *HDAC5* and *Ccl2* escapers by western blot analysis. The iKPC tumors were used as control. **D**, Gates of macrophages, monocytes and neutrophils in a representative iKPC tumor and a *HDAC5* escaper tumor generated from orthotopic allograft models in C57BL/6 mice by FACS analysis. Data are displayed by FlowJo. **E**,

CyTOF analysis of immune cell subtypes in iKPC-5 primary tumors (n = 5) and *HDAC5* escaper tumors (n = 4) generated from orthotopic allograft models in C57BL/6 mice. Two-tailed unpaired t tests were performed to calculate the p values. **F,** Validation of SMAD4 knockout in iKPC-5 cells by western blot analysis. For **B** and **E**, data are represented as mean ± SEM.